On Coordination and Stabilization of Two Xerographic Printers

Teck Ping Sim, and Perry Y. Li

Abstract— The problem of coordinating and stabilizing the two color tone reproduction curves (TRC) of two xerographic printing engines is considered. This problem is critical to enable two printers to print the same image/collection of images in parallel, hence speeding the overall printing process. The proposed control systems use a small number of actuators and a small number of measurements to coordinate and stabilize the potentially high-dimensional TRC of the two printers. The goal for TRC coordination and stabilization is to minimize the overall least squares deviation of the two TRCs and the overall least squares deviation of each of the TRCs from the nominal subject to disturbances on the printers. In this paper an optimal static and robust static controllers are proposed to stabilize and coordinate the potential high dimensional TRC. Simulations and experiments validate the efficacy of the proposed controllers.

I. INTRODUCTION

Maintaining colors/tones consistency despite variation in media properties, materials, environment and other disturbances is a very important print quality attribute of digital printers/copiers. In tasks requiring printing large quantities of the same image or collection of images with multiple printers, maintaining printer-to-printer colors/tones consistency is as important as page-to-page consistency. This is because if the printers are left uncoupled (i.e. maintaining the colors/tones consistency from printers-to-printers is not considered), then prints from one printer to another may appear different although the page-to-page consistency is maintained. In this paper we proposed control approaches to coordinate the tone responses of two xerographic printers subject to differing levels of disturbances.

A digital color xerographic printer generates color by printing and overlaying the Cyan, Magenta, Yellow and blacK (CMYK) separations. The printing of each color separation is characterized by the tone reproduction curve (TRC), TRC : $[0, 1) \rightarrow \Re$, desired tone $\mapsto$ output-tone, where the tone `tone` of the separation is the solidness of the primary toner color. For example, a patch with `tone` = 0.1 for the magenta color separation corresponds to a light violet whereas `tone` = 1.0 corresponds to solid magenta color. Physically, the tone of the primary separations are determined by the pattern and size of the half tone dots printed. Roughly speaking, the denser and bigger the dots are, the more solid the color. The final color printed is a composition of the colors of the individual separation. Thus, the so called Image Output Terminal (IOT) portion of the printer can be considered a mapping IOT : $(\text{tone}_C, \text{tone}_Y, \text{tone}_M, \text{tone}_K) \mapsto$ output-color where $(\text{tone}_C, \text{tone}_Y, \text{tone}_M, \text{tone}_K)$ are the

tones for the four color separations. Hence, the control objective here is to coordinate and stabilize the TRC of each separation. If the manner in which the primary color separations are combined is stable and constant, then the output color will also be consistent when the TRC for each separation has been effectively coordinated and stabilized. The TRC control formulations pose significant problems for sensing and control. It is because the TRC, as mappings, are potentially infinite dimensional whereas only a small number of actuators and sensors are available. Even when each color coordinate is modestly discretized into 16 steps, the color quality of $16^3 = 4096$ desired colors need to be kept track of for the color control problem, and 16 tones must be kept track of for the TRC control problem for each separation.

The stabilization of the TRC has been studied in our previous paper [1], [2]. While coordination control of electromechanical systems has been well developed and matured [3], to the best of our knowledge there are no reported works on applying this to the coordination of the TRC of different print systems.

An optimal static control approach and a robust static control approach are proposed for coordinating and stabilizing the TRCs. Without loss of generality, consider the case of two printers. The main idea here is to ensure that the TRC of printer 1 and 2 are close to their nominal (for stabilization) and to each other (for coordination) in a least square sense. However since the number of tones to stabilize and coordinate is potentially high, and the there are only small number of effective actuators, there maybe loss of stabilization performance with increase in coordination. In our case, coordination performance may sometime be more important than in stabilization (i.e. tracking the individual tones of each printers) because maintaining printer-to-printer prints consistency maybe more desirable. As given in [1], a dynamic realization of the static controller is used that ensure close loop stability and achieves the same steady-state performance as the given static controller (i.e. optimal static or robust static control approach).

The rest of this paper is organized as follows. In Section II, the xerographic printing process is briefly described. The TRC coordination and stabilization problem is formulated in Section III. In Section IV, the optimal static and robust static controller are presented. Section V contains simulation results and Section VI gives discussion on the experiment results. Finally, Section VII contains some concluding remarks.

II. THE XEROGRAPHIC PRINTING PROCESS

In this section, a brief description of a single xerographic control system is given (see [4] for details). The digital xerographic printing process revolves around the photoreceptor, which is usually a drum/belt that continuously rotates and cylindrically interacts with several stationary subsystems as
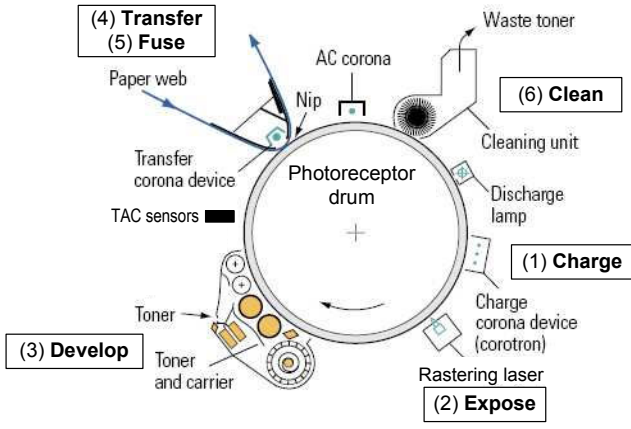
Fig. 1. Schematic of a typical single tone xerographic marking process

shown in Fig. 1. The photoreceptor acts as an image carrier where a toner image is first built up before being transferred to paper. The density profile of the toner image, which is critical to the print quality, depends on the behavior of the following steps: (1) Charging is the first step in the xerographic process. In this step a corona discharged from a high voltage corotron wire causes air to breakdown into charged particles, showering the photoreceptor with a *uniform charge density*. (2) Exposure is the next step where light produced by the binary operated raster laser beam scans the photoreceptor line by line to discharge the normally charged photoreceptor. This creates on the photoreceptor a *latent image* resembling the desired image. The depth of discharge is affected by the laser power according to the nonlinear Photo-Induced Discharged Characteristics (PIDC) of the photoreceptor. (3) Development involves selectively depositing charged toner particles on the latent image of the photoreceptor by virtue of the bias voltage of the development housing and the photoreceptor. (4) Transfer involves depositing loosely attached toner particles on the photoreceptor onto paper. (5) Fusing enables the image to be permanently fixed on paper by melting the plastic coating of the toner particles on the paper surface with high pressure and temperature. (6) The photoreceptor is discharged and cleaned of any excess toner using coronas, lamps, brushes, and/or scraper blades. Residual toner will otherwise contaminate the next latent image that the photoreceptor will generate.

From the xerographic process descriptions, to maintain the print consistency, it is critical that the charge density on the photoreceptor, the electrostatic adhesion force, the cleaning process, etc. need to be consistent for every print. Subject to uncontrollable changes (material, temperature, humidity, etc.), this is difficult to achieve even with the most well designed xerographic marking process. Typically these print variations are slow varying, often not measured, and their effects on the TRC cannot be easily characterized and vary from printer-to-printer. In addition, the xerographic process is nonlinear and uncertain, and the manufactured units on the production line vary from unit to unit.

Fortunately there are several parameters that can be adjusted to compensate for the print variations to maintain the print consistency. These include the voltage across the corotron wire in the charging stage, the laser power in the exposing stage and the bias development voltage in the developing stage. Typically, about three to five xerographic actuators are available.

III. PROBLEM FORMULATION

Let $TRC_\ell(k) : [0,1) \to \Re$ be the time-varying TRC of the ℓ-th printing process where k is the time index (or belt or print cycle index). It maps the desired input tone to the printed output tone. Although the TRC is potentially infinite dimensional, we assume that the TRC can be adequately described by its values at M_ℓ uniformly distributed tones, $\texttt{tone}_i \in [0,1)$, $i = 1, \ldots, M_\ell$, where $M_\ell >> 1$ can be fairly large, i.e.

$$TRC_\ell(k) = \begin{pmatrix} TRC_\ell(k)[\texttt{tone}_1] \\ \vdots \\ TRC_\ell(k)[\texttt{tone}_{M_\ell}] \end{pmatrix} \in \Re^{M_\ell}$$

As noted in [1], in the presence of xerographic control inputs and disturbances, the possibly nonlinear TRC can be represented by the static, linear time varying, uncertain model as follows:

$$TRC_\ell(k) = \widehat{\phi}_\ell(I + \Delta_\ell(k)W_{u_\ell})\bar{u}_\ell(k) + TRC_\ell^* + \bar{d}_\ell(k) \quad (1)$$

where $u_\ell(k) \in \Re^m$ are the xerographic actuators, $TRC_\ell^* \in \Re^{M_\ell}$ is the nominal TRC, and $\bar{d}_\ell(k) \in \Re^{M_\ell}$ is a slowly time varying disturbance. In addition, $\widehat{\phi}_\ell \in \Re^{M_\ell \times m_\ell}$ is the nominal sensitivity function, $\Delta_\ell(k) \in \Re^{m_\ell \times m_\ell}$ is the multiplicative uncertainty, $W_{u_\ell} \in \Re^{m_\ell \times m_\ell}$ is the matrix of given uncertainty weights. In this paper, it is assumed that the xerographic system have a relatively good degree of control to compensate for the disturbances on the TRC. Also, $\bar{u}_\ell(k) := u_\ell - u_{o_\ell}$, where u_{o_ℓ} is the nominal control input.

Sensing of the $TRC_\ell(k) \in \Re^{M_\ell}$ at time instant k is achieved by printing and measuring $n_\ell << M_\ell$ tones in the form of small test patches. The number of n_ℓ samples will be determined by the number of available sensors, as well as the productivity and materials cost of printing the test patches. In our previous papers [2], [5], [6], a time-sequential sampling approach is proposed to sample the time-varying TRC. In this approach, n_ℓ different tones are sampled at different time k. Which tones are printed at what times are determined by the $M_\ell/n_\ell-$ periodic time-sequential sampling pattern. A Kalman reconstruction is then used to recover the time-varying TRC with minimal reconstruction errors. Hence, we assume here that an approximate $TRC_\ell(k)$ is available at each time-step, k.

The stabilization control objective is for the TRC to match the desired nominal TRC, TRC_ℓ^* at each $\texttt{tone}_i, i = 1, 2, \ldots, M_\ell$, as $k \to \infty$

$$TRC_\ell(k)[\texttt{tone}_i] \to TRC_\ell^*[\texttt{tone}_i]$$

Without loss of generality, consider two printer. Then the coordination control objective is for the TRC of printer 1 to match the TRC of printer 2 at each selected q tones, $\texttt{tone}_i, i = 1, 2, \ldots, q$, as $k \to \infty$

$$TRC_1(k)[\texttt{tone}_i] \to TRC_2(k)[\texttt{tone}_i]$$

While it is true that if exact stabilization is achieve, then the coordination objective is similarly achieved, this is typically not attainable. This is because the number of tones to stabilize and coordinate is potentially high, and there are only small number of effective actuators. Hence there maybe loss of stabilization performance with increase in coordination and vice versa. Therefore, emphasis must be given to stabilization or coordination as deemed necessary. In our case, coordination performance may sometime be more important than in stabilization because maintaining printer-to-printer prints consistency maybe more desirable.

IV. TRC COORDINATION AND STABILIZATION CONTROLLER DESIGN

In this section, we consider the design of the TRC coordination and stabilization controller considering two xerographic print systems i.e. $\ell = 1, 2$ in (1). Let,

$$\bar{e}_1(k) = TRC_1(k) - TRC_1^* \tag{2}$$
$$\bar{e}_2(k) = TRC_2(k) - TRC_2^* \tag{3}$$

First, an optimal static control approach is developed by neglecting the system uncertainty $\Delta_\ell(k)$ in (1). Then, a robust static control approach is developed that accounts for the system uncertainty.

A. Optimal Static Control Approach

The high dimensionality of the TRC coupled with limited actuation capabilities do not permit us to control all tones of both printers. An optimal control approach is proposed here to ensure that $TRC_1(k)$ and $TRC_2(k)$ are close to their nominal i.e. TRC_1^* and TRC_2^* respectively (for stabilization) and to each other (for coordination) in a least squares sense. In this section, we temporarily ignore system uncertainty in (1), i.e. $\Delta_1(k) = 0$ and $\Delta_2(k) = 0$.

Let $\epsilon(k)$ denotes the coordination error

$$\epsilon(k) = H_1 \bar{e}_1(k) - H_2 \bar{e}_2(k) \tag{4}$$

where $H_1 \in \Re^{q \times M_1}, H_2 \in \Re^{q \times M_2}$ give the interpolation matrices such that we pick collection of q-tones to be coordinated. Hence, the optimal control problem is to find the control $\bar{u}(k) := [\bar{u}_1(k), \bar{u}_2(k)]^T \in \Re^{m_1 + m_2}$ based on the approximate TRC of both printer, $TRC_1(k)$ and $TRC_2(k)$, such that the following quadratic performance index (QPI), $J(k)$ is minimized.

$$J(k) = \frac{1}{2} \bar{e}_1^T(k) Q_1 \bar{e}_1(k) + \frac{1}{2} \bar{e}_2^T(k) Q_2 \bar{e}_2(k) + \frac{1}{2} \epsilon^T(k) S \epsilon(k) + \frac{1}{2} \bar{u}_1^T(k) R_1 \bar{u}_1(k) + \frac{1}{2} \bar{u}_2^T(k) R_2 \bar{u}_2(k) \tag{5}$$

where $Q_1 \in \Re^{M_1 \times M_1}, Q_2 \in \Re^{M_2 \times M_2}, S \in \Re^{q \times q}, R_1 \in \Re^{m_1 \times m_1}$ and $R_2 \in \Re^{m_2 \times m_2}$ are weighting matrices. Let $\bar{d}(k) = [\bar{d}_1(k), \bar{d}_2(k)]^T \in \Re^{M_1 + M_2}$. A term expressing the coordination objective (weighted by the weighting matrix, S) was explicitly introduced in the performance index. Substituting (2)-(4) into (5), we have:

$$J(k) = \frac{1}{2} \bar{u}^T(k) G_1 \bar{u}(k) + \frac{1}{2} \bar{d}^T(k) G_2 \bar{d}(k) + \frac{1}{2} \bar{u}^T(k) G_3 \bar{d}(k) + \frac{1}{2} \bar{d}^T(k) G_3^T \bar{u}(k) \tag{6}$$

where

$$G_1 = \begin{pmatrix} \widehat{\phi}_1^T Q_1 \widehat{\phi}_1 + \widehat{\phi}_1^T H_1^T S H_1 \widehat{\phi}_1 + R_1 & -\widehat{\phi}_1^T H_1^T S H_2 \widehat{\phi}_2 \\ -\widehat{\phi}_2^T H_2^T S H_1 \widehat{\phi}_1 & \widehat{\phi}_2^T Q_2 \widehat{\phi}_2 + \widehat{\phi}_2^T H_2^T S H_2 \widehat{\phi}_2 + R_2 \end{pmatrix}$$

$$G_2 = \begin{pmatrix} Q_1 + H_1^T S H_1 & -H_1^T S H_2 \\ -H_2^T S H_1 & Q_2 + H_2^T S H_2 \end{pmatrix}$$

$$G_3 = \begin{pmatrix} \widehat{\phi}_1^T Q_1 + \widehat{\phi}_1^T H_1^T S H_1 & -\widehat{\phi}_1^T H_1^T S H_2 \\ -\widehat{\phi}_2^T H_2^T S H_1 & \widehat{\phi}_2^T Q_2 + \widehat{\phi}_2^T H_2^T S H_2 \end{pmatrix}$$

Taking the derivative with respect to $\bar{u}^T(k)$ we have:

$$\frac{\partial J(k)}{\partial \bar{u}^T(k)} = G_1 \bar{u}(k) + G_3 \bar{d}(k)$$

Then taking $\partial J(k)/\partial \bar{u}^T(k) = 0$ we have:

$$\bar{u}(k) = (G_1^T G_1)^{-1} G_1^T G_3 \bar{d}(k)$$

Let $K := (G_1^T G_1)^{-1} G_1^T G_3$ and $\widehat{\phi} = \begin{pmatrix} \widehat{\phi}_1 & 0 \\ 0 & \widehat{\phi}_2 \end{pmatrix}$. Hence, we have:

$$\bar{u}(k) = K_{opt} \bar{e}(k) \tag{7}$$

where $K_{opt} = (I + K\widehat{\phi})^{-1} K \in \Re^{(m_1 + m_2) \times (M_1 + M_2)}$ and $\bar{e}(k) = [\bar{e}_1(k), \bar{e}_2(k)]^T$. Notice that (7) is a linear feedback of the error.

B. Static Robust Control Approach

In this section, the system uncertainty $\Delta(k)$ is taken into account. From (1)-(3) we have:

$$\bar{e}(k) = \widehat{\phi}[I + \Delta(k) W_u] \bar{u}(k) + \bar{d}(k) \tag{8}$$

where $\bar{e}(k) = [\bar{e}_1(k), \bar{e}_2(k)]^T$, $\widehat{\phi} = \begin{pmatrix} \widehat{\phi}_1 & 0 \\ 0 & \widehat{\phi}_2 \end{pmatrix}$, $\Delta(k) = \begin{pmatrix} \Delta_1(k) & 0 \\ 0 & \Delta_2(k) \end{pmatrix}$, and $W_u = \begin{pmatrix} W_{u_1} & 0 \\ 0 & W_{u_2} \end{pmatrix}$. Note that $\Delta(k)$ and $\bar{d}(k)$ are unknown.

Let $U(z) = K(z)E(z)$ where $K(z)$ is some linear feedback controller to be specified. Define the error weighting $W_{e_1} \in \Re^{M_1 \times M_1}, W_{e_2} \in \Re^{M_2 \times M_2}$ which specify the relative importance of the TRC error at different tones and the coordination error weighting $W_{c_1} \in \Re^{M_1 \times M_2}$ together with $W_{c_2} \in \Re^{M_2 \times M_1}$ to specify the relative importance of the TRC coordination at different tones. We define the coordination and stabilization error metric as:

$$\begin{pmatrix} W_{e_1} \bar{e}_1(k) + W_{c_1} \bar{e}_2(k) \\ W_{c_2} \bar{e}_1(k) + W_{e_2} \bar{e}_2(k) \end{pmatrix} = W_{ce} e(k)$$

where $W_{ce} = \begin{pmatrix} W_{e_1} & W_{c_1} \\ W_{c_2} & W_{e_2} \end{pmatrix} \in \Re^{(M_1 + M_2) \times (M_1 + M_2)}$. The closed loop system can be expressed as a linear fractional transformation(LFT) as in Fig. 2. Specifically, we have:

$$\begin{pmatrix} w \\ W_{ce}\bar{e} \\ e \end{pmatrix} = \begin{pmatrix} 0 & 0 & W_u \\ W_{ce}\widehat{\phi} & W_{ce} & W_{ce}\widehat{\phi} \\ \widehat{\phi} & I & \widehat{\phi} \end{pmatrix} \begin{pmatrix} v \\ \bar{d} \\ \bar{u} \end{pmatrix}$$

with feedback connection $v(k) = \Delta(k)w(k)$ and $U(z) = K(z)E(z)$. Because of the static nature of the xerographic
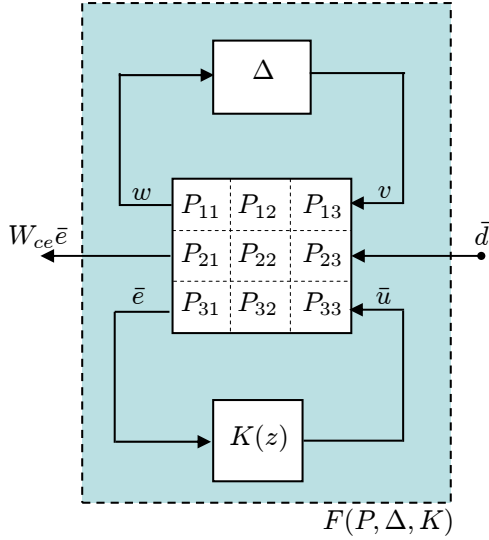
Fig. 2. LFT representation of linear system model

process, and the xerographic disturbances are generally slowly varying, the performance optimization is restricted to the steady-state case. Hence, since $W_{ce}\bar{e}^{\infty}$ is linear w.r.t $\bar{d}^{\infty}$, there exists some matrix, $F(P, \Delta^{\infty}, K^{\infty})$ s.t.

$$W_{ce}\bar{e}^{\infty} = F(P, \Delta^{\infty}, K^{\infty}) \cdot \bar{d}^{\infty}$$

The goal here is to find a controller $K(z)$ such that for the worst case performance and for as large a class of uncertainty $\Delta(\cdot)$ as possible, $\|F(P, \Delta^{\infty}, K^{\infty})\|_2$ is minimized. This is achieved by optimizing the following steady-state performance index:

$$\bar{\gamma}(K^{\infty}) = \min \left\{ \gamma : \sup_{\|\Delta^{\infty}\| \leq \frac{1}{\gamma}} \bar{\sigma}(F(P, \Delta^{\infty}, K^{\infty})) \leq \gamma \right\}$$

where $\bar{\sigma}[\cdot]$ denotes the maximum singular value of its argument. Hence, the optimal controller dc gain is

$$K_{rob} := \arg \min_{K^{\infty}} \bar{\gamma}(K^{\infty})$$

Finding K_{rob} can be achieved by procedure described in [1], [7]. Hence the controller is given by:

$$\bar{u}(k) = K_{rob}\bar{e}(k) \tag{9}$$

C. Realizing TRC stabilization and coordination controller[1]

In (7) and (9), $\bar{u}(k) = K_{opt}\bar{e}(k)$ and $\bar{u}(k) = K_{rob}\bar{e}(k)$ are not realizable because $\bar{e}(k)$ is not available until $\bar{u}(k)$ is given. Instead, let the realization of the controller be of the form:

$$\bar{u}(k+1) = A\bar{u}(k) + B\bar{e}(k) \tag{10}$$

Let K_{dc} denotes K_{opt} or K_{rob} depending on which control approach being used. Hence the controller will have a sub-optimal dc gain if

$$K_{dc} = (I - A)^{-1}B \tag{11}$$

and the nominal stability of the closed-loop system [i.e. $\Delta(k) = 0$] is given by:

$$|\text{eig}(A + B\widehat{\phi})| < 1 \tag{12}$$

Let $L = K_{dc}\widehat{\phi}$ be the nominal loop gain. By conditions (11) and (12), we have $A_c = A + B\widehat{\phi} = L + A(I - L)$. Hence, given that A_c is a stable closed-loop matrix (picked by the designer), we can find the A and B matrices from the dynamic controller as follows:

$$A = (A_c - L)(I - L)^{-1}$$
$$B = (I - A)K_{dc}$$

V. SIMULATION EXAMPLE

The behavior of the xerographic plant is simulated by taking the family of linear plants with uncertainty of the form (1) for both printer $\ell = 1$ and $\ell = 2$. Here, we consider the uncertainty $\Delta_{\ell}(k)$ of the form:

$$\Delta_{\ell}(k)W_{u_{\ell}} = \delta_{\ell}\Delta_{\ell}$$

where Δ_{ℓ} is randomly chosen with $\|\Delta_{\ell}\| = 1$ and $\delta_{\ell} \in \Re$ systematically varied. $\widehat{\phi}_{\ell}$ is obtained by least square fitting of a set of nominal experimental data (i.e. at $\Delta_{\ell}(k) = 0$). In the following simulation, we assume $\widehat{\phi}_1 = \widehat{\phi}_2$. In this simulation example we have picked $M_1 = M_2 = 39$ number of tones, $q = 10$ number of tones to coordinate and $m_1 = m_2 = 3$ number of actuators of the xerographic printing process. The weighting matrices are arbitrarily chosen to be $W_{u_1} = 0.1I$ and $W_{u_2} = 0.1I$.

The TRC disturbances, $\bar{d}_{\ell}(k)$ is modeled as follows:

$$\bar{d}_{\ell}(k) = [\Lambda_{\ell}\lambda_{\ell}(k) + \bar{b}_{\ell}] + \Gamma_{\ell}\gamma_{\ell}(k) \tag{13}$$

where $k \in \mathcal{Z}^+$ is the index. $\Lambda_{\ell}\lambda_{\ell}(k) + \bar{b}_{\ell}$ gives the large-magnitude, low frequencies TRC variations with $\Lambda_{\ell} \in \Re^{M_{\ell} \times M_{\ell}}$ denoting the tonal basis function, $\lambda_{\ell}(k) \in \Re^{M_{\ell}}$ gives time-varying coefficients (modeled by an integrator dynamics) and $\bar{b}_{\ell} \in \Re^{M_{\ell}}$ is a constant bias vector. $\Gamma_{\ell}\gamma_{\ell}(k)$ gives the small-magnitude, high frequencies variations with $\Gamma_{\ell} \in \Re^{M_{\ell} \times M_{\ell}}$ denoting the matrix of the Fourier basis functions and $\gamma_{\ell}(k) \in \Re^{M_{\ell}}$ is the vector of Fourier coefficients representing the tonal frequency content of the disturbance (modeled by a pink noise dynamics). We further assume that all the M_{ℓ} tones of the TRC are known at each time-step, k either by directly sampling these M_{ℓ} tones or by using the time-sequential sampling approach where small number of n_{ℓ} tones are sampled and then reconstructed with a periodic Kalman filter. For details of the disturbance modeling and Kalman reconstruction filter, see our previous papers in [5], [6].

The TRC error norm, $\|\bar{e}_{\ell}(k)\|_2$ and coordination error norm, $\|\epsilon(k)\|_2$ are used as the measures of the the stabilization and coordination performance at each time-step, k respectively. The time-normalized mean square TRC error,

$$\text{MSE-STAB-}\ell_L = \left[\frac{1}{L} \sum_{k \in [l_0, l_0+L]} \|\bar{e}_{\ell}(k)\|_2^2 \right]^{\frac{1}{2}}$$

and the time-normalized mean square coordination error,

$$\text{MSE-COORD}_L = \left[\frac{1}{L} \sum_{k \in [l_0, l_0+L]} \|\epsilon(k)\|_2^2 \right]^{\frac{1}{2}}$$
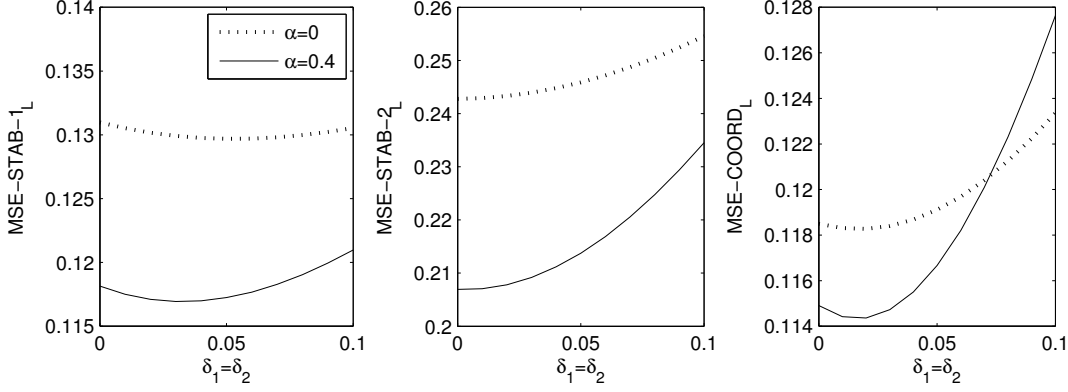
3340

Fig. 3. Stabilization and coordination performance using the robust static control approach of printer 1 and 2 with different uncertainty level given by different settings of $\delta_1 = \delta_2$.

are used as measures of the overall stabilization and coordination performance respectively.

In both the optimal static and robust static control design considered here, we pick the stable closed-loop matrix, $A_c = \text{diag}(0.5, 0.5, 0.5, 0.5, 0.5, 0.5)$ and no sensing noise is assumed. First, consider the optimal static controller. The stabilization weighting matrices, Q_1 and Q_2 are pick such that greater emphasis is given for the lower density tones as the human visual system are more sensitive to the variations of these tones. We pick $Q_1 = W_{e_1}^T W_{e_1}$ where

$$W_{e_1} = \text{diag}([1 : -0.2/(M_1 - 1) : 0.8] \cdot \wedge 3) \qquad (14)$$

in Matlab's notation and $Q_2 = Q_1$. Let $R_1 = 1 \times 10^{-6}I, R_2 = 1 \times 10^{-6}I$. With no uncertainty (i.e. $\delta_1 = 0, \delta_2 = 0$), MSE-COORD$_L$ using $l_0 = 500, L = 500$ are 0.1242 and 0.1030 for $S = 0$ (no coordination) and $S = 10I$ (with coordination) respectively. However, the optimal static control is not designed for condition where there is uncertainty in the identification of the plant model. Imposing uncertainty (i.e. $\delta_1 = \delta_2 = 0.1$), MSE-COORD$_L$ deteriorate to 0.1601 with coordination ($S = 10I$). To address this the robust static control approach is used. We pick W_{e_1} as given in (14) and $W_{e_2} = W_{e_1}$. The coordination weighting matrices are given by $W_{c_1} = \alpha H_1^T H_2$, $W_{c_2} = \alpha H_2^T H_1$ where increasing $\alpha \in \Re$ enable greater emphasis on coordination. We consider two different setting of α i.e. $\alpha = 0, 0.4$.

Fig. 3 shows the MSE-STAB-1$_L$, MSE-STAB-2$_L$ and MSE-COORD$_L$ performance metric with different level of uncertainty given by $\delta_1 = \delta_2$. With no uncertainty, a small coordination error(i.e. small MSE-COORD$_L$ value) can be maintained using $\alpha = 0.4$ at the expense of robustness. In this case, robustness can be regained with a loss in stabilization and coordination performance by setting α to be small. Hence, appropriate settings W_u and W_{ce} need to be selected to obtained the best tradeoff between robustness and performance.

VI. EXPERIMENTS

The proposed TRC stabilization and coordination system was experimentally tested using a Xerox Phaser 7700 xerographic printer as both printer 1 and 2. A X-rite DTP70
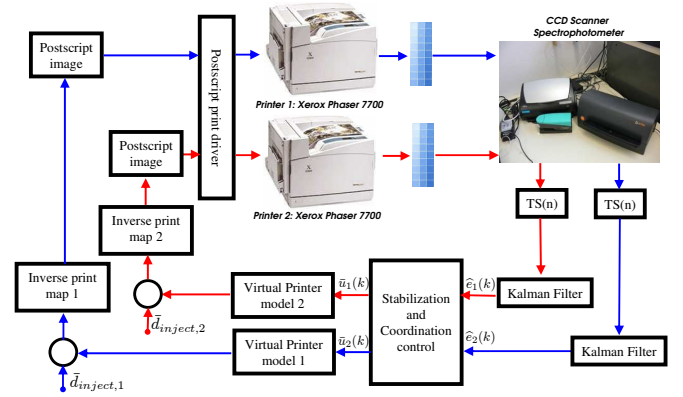

Fig. 4. Experimental setup for sensing and control for stabilization and coordination of the TRCs

scanning spectrophotometer is used to measured the printed tone patches. Fig. 4 shows the schematic of our setup. We do not have direct access to the xerographic actuators. To evaluate the proposed TRC stabilization control system, a virtual printer model is used to generate the response (color image) due to changes in the actuator inputs $[\bar{u}_\ell(k)$ in (1)]. The virtual printer model is given by (1) with no disturbance $[\bar{d}_\ell(k) = 0]$ and no plant perturbation $[\Delta_\ell(k) = 0]$. By calibrating the printers such that it is an identity map at nominal, we can capture the effect of the disturbances/uncertainty on the TRC stabilization system. In our case study, the output response is in the form of a single colorant wedge of 39 different tones. Since the inherent print process disturbances is slow varying, we can speed up this process by artificially injecting a simulated disturbance source $\bar{d}_{inject,\ell}(k)$ as given by (13). In this experiment, the injected disturbance for printer 1 and 2 are selected (by appropriately selecting the process noise covariance and frequency content of $(\lambda_\ell(k), \gamma_\ell(k))$ and the constant bias vector, $\bar{b}_\ell$) such that a visually significant color tone difference is observed between the two printers.

Fig. 5 shows the TRC stabilization and coordination performance for three cases (1) no stabilization and coordination control; (2) stabilization and no coordination and (3) stabi-
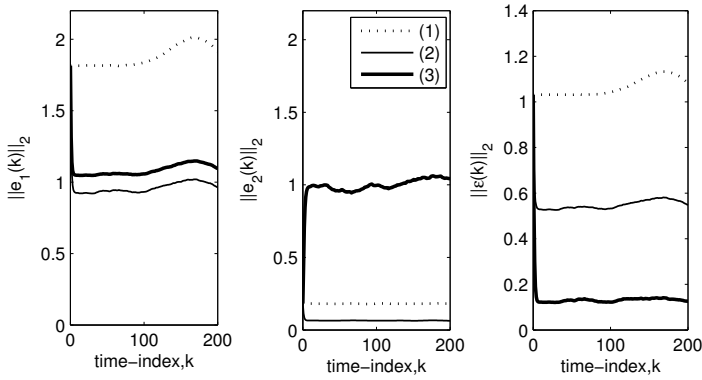
Fig. 5. Experimental TRC stabilization and coordination performance with optimal $TS(1)$ sampling of printer 1 and 2.
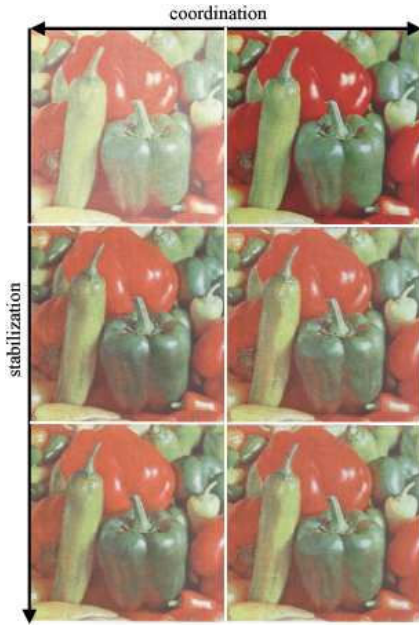

Fig. 6. Color image printout of printer 1(left) and printer 2(right) at different time-step, k for the optimal static control approach *with* coordination. Note that color prints at $k = 25$ and $k = 50$ are much more closer to each other than with print at $k = 0$ indicating stabilization of the color prints; and color prints at $k = 50$ of both printers are closer than than given at $k = 0$ indicating coordination.
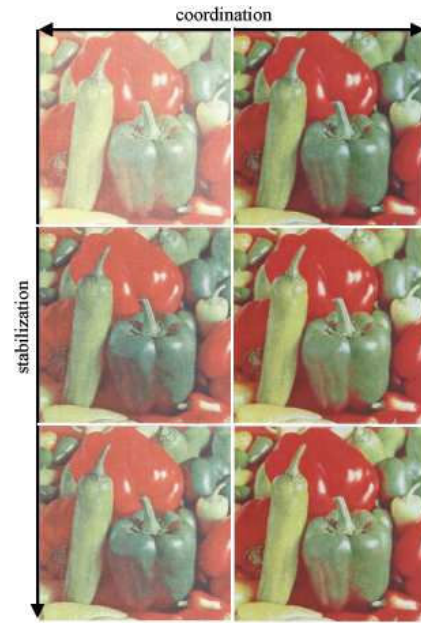

Fig. 7. Color image printout of printer 1(left) and printer 2(right) at different time-step, k for the optimal static control approach *without* coordination. Note that, color prints at $k = 25$ and $k = 50$ are much more closer to each other than with print at $k = 0$ indicating stabilization of the color prints; and color prints at $k = 50$ of both printers are mismatch indicating a lack of coordination.

lization and coordination using the optimal static controller and the optimal $TS(1)$ sampling [6]. Effective stabilization and coordination is demonstrated with option (3). When this stabilization and coordination process is repeated for all the primary CMY primary colorants, we are able to achieve good color coordination between the two printer as shown in Fig. 6 as oppose to the case without coordination as shown in Fig. 7.

VII. CONCLUSION

An optimal and robust static TRC stabilization and coordination control system has been proposed. The controller is designed assuming availability of $TRC_\ell(k)$ of all printers (can be fulfilled using the time-sequential sampling approach proposed in our previous papers [5], [6]) and with

the availability of small number of effective xerographic actuators. Simulation and experimental results confirmed that stabilization and coordination can be achieved with the proposed controllers. Given the uncertainty in the plant identification and the fact that manufactured units on the production line vary from unit to unit, the robust control approach can be used to gain the best tradeoff between coordination/stabilization performance and robustness.

REFERENCES

[1] P.Y.Li and S.A.Dianat, "Robust stabilization of tone reproduction curves for xerographic printing process," *IEEE Transactions on Control Systems Technology*, vol. 9, no. 2, pp. 407–415, 2001.

[2] T.P.Sim, P.Y.Li, and D.J.Lee, "Using time-sequential sampling to stabilize the color and tone reproduction functions of a xerographic printing process," *IEEE Trans. on Control Systems Technology*, vol. 15, no. 2, pp. 349–357, March 2007.

[3] M.Tomizuka, J.S.Hu, and T.C.Chiu, "Synchronization of two motion control axes under adaptive feedforward control," *Trans. of the ASME*, vol. 114, pp. 196–203, June 1992.

[4] L.B.Schein, *Electrophotography and Development Physics*. Springer-Verlag, 1992.

[5] P.Y.Li, T.P.Sim, and D.J.Lee, "Time-sequential sampling and reconstruction of tone and color reproduction functions for xerographic printing," in *Proceedings of the 2004 American Control Conference*, Boston, United States, June 2004, pp. 2630–2635.

[6] T.P.Sim and P.Y.Li, "Optimal time sequential sampling of tone reproduction function," in *Proceedings of the 2006 American Control Conference*, Minneapolis, United States, June 2006, pp. 5728–5733.

[7] R.Smith and A.Packard, "Optimal control of perturbed linear static systems," *IEEE Trans. on Automatic Control*, vol. 41, no. 4, pp. 579–584, April 1996.